Supplementary Material

Dynamic insights on transcription initiation and RNA processing during bacterial adaptation

Caroline Lacoux[1,#], Aymeric Fouquier d'Hérouël[2], Françoise Wessner- Le Bohec[1], Nicolas Innocenti[1,3,#], Chantal Bohn[4], Sean P. Kennedy[5,#], Tatiana Rochat[6], Rémy A. Bonnin[4,#], Pascale Serror[1], Erik Aurell[3,7], Philippe Bouloc[4] and Francis Repoila[1,*]

Email adresses: CL: lacoux@ipmc.cnrs.fr, AFD: aymeric.dherouel@uni.lu, FW: francoise.le-bohec@inra.fr, NI: nicolas@innocenti.se, CB: chantalbohn@gmail.com, SPK: sean.kennedy@pasteur.fr, TR: tatiana.rochat@inra.fr, RB: remy.bonnin@u-psud.fr, PS: pascale.serror@inra.fr, EA: eaurell@kth.se, PB: philippe.bouloc@i2bc.paris-saclay.fr, FR: francis.repoila@inra.fr

Corresponding author : francis.repoila@inra.fr

Running head: Dynamics of transcription initiation and RNA processing

This file contains:

Section S1: Dynamics of RNA levels in response to σ^E induction (Contains Figures S1 and S2).

Section S2: Assignment of 5' RNA ends.

Section S3: **Figure S3**. Patterns of changes in TIF at σ^E-TSSs assigned as UNDs or PSSs in this study.

Figure S4. Examples of changes in TIF at σ^E-independent TSSs

Section S4: RNA dynamics at the *bepA-yfgD* operon (Contains Figures S5)

References

Section S1:

Dynamics of RNA levels in response to σ^E induction

Global view of the evolving transcriptome

Our experimental system consisted of a plasmid (pZE21-rpoE) that harbor the σ^E encoding sequence under control of the inducible promoter $P_{LtetO-1}$ in *E. coli* K12 strain MG1655 (Fig. S1A). It was previously shown that upon the addition of anhydrotetracyline (aTc), a $P_{LtetO-1}$ inducer, σ^E amounts increase 5 to 10-fold compared to levels at t_0 (Bury-Mone et al. 2009). To observe the reshaping of the RNA landscape within bacteria sensing and responding to aTc, total RNA was collected every 5 minutes (min) during 20 min, a sampling period deliberately shorter than the doubling time of the bacterial strain (Bury-Mone et al. 2009). The experiment was performed with three independent clones, and RNA samples were analyzed by tagRNA-seq (Fig. 1A) (Innocenti et al. 2015). RNA-seq raw data were processed as presented in the main manuscript and compiled in Supplemental Tab. S1. As control of σ^E induction from the plasmid system, we observed a drastic increase of *rpoE* mRNA (> 60-fold) within the first 5 min after addition of aTc, indicating that the amount of *rpoE* mRNA was successfully increased by the inducer. Over the course of the experiment, *rpoE* RNA levels remained between 60- and 100-fold higher than levels measured at t_0 (Tab. S2).

We then focused on major temporal changes by selecting transcripts whose levels varied at least 4-fold compared to their original abundance at t_0. By imposing such a threshold, 701 coding sequences (CDSs) were selected, and we distinguished the temporal expression pattern of selected CDSs (Fig. 1B, Tab. S2):

i) RNAs that reached the imposed threshold at t_5.

ii) RNAs that reached the threshold after t_5. For those, three expression patterns were observed:

a) RNAs that followed the same trend as observed during the interval $t_{5\text{-}0}$, but whose levels reached the threshold imposed at a slower pace (increased or decreased levels). These CDSs were considered as 'changing at t_5'.

b) RNAs that displayed 'transient' expression patterns, i.e. featuring increased/decreased levels during the first 5 to10 min (i.e. within intervals $t_{5\text{-}0}$ or $t_{10\text{-}0}$), and then reversed their expression pattern. These CDSs were considered as changing at t_5 or t_{10} (e.g. *ahpF*, Fig. S1B).

c) RNAs with late onset variation, e.g. an RNA selected at t_{15}, whose levels did not show significant variation during the time interval $t_{10\text{-}0}$.

Thus, we established a time-specific expression pattern during the adaptation process triggered by the σ^E induction. The majority (~90%) of CDSs were selected within the first 10 min of the kinetics (~50% and ~41% at t_5 and t_{10}, respectively). In sharp contrast, only ~10% displayed significant changes afterwards (~8% and ~2 % at t_{15} and t_{20}, respectively), (Fig. 1B, Tab. S2). Furthermore, CDSs reported or predicted σ^E-dependent were expected to rank among the first to respond since the adaptation process resulted from the σ^E induction (Keseler et al. 2017). Indeed, we observed their decreasing proportion within the pool of selected CDSs at each experimental time point: Nearly one third of these CDSs were selected at t_5 (102 out of 350 total), less than 15% at t_{10} (39 out of 285), and no σ^E-dependent CDS was retrieved at t_{15} and t_{20} (Fig. 1B, Tab. S2). This data also indicated that most likely changes in RNA levels for σ^E-independent CDSs were a consequence of the σ^E

induction and highlighted the coordinated expression between the σ^E regulon and other regulons in *E. coli*, agreeing with previous reports (Fig. S1C, S1D, S1E) (Rhodius et al. 2006; Bury-Mone et al. 2009; Rhodius and Mutalik 2010; Gogol et al. 2011). Expression levels of CDSs selected at t_{20} and whose RNA levels specifically change at $t_{20\text{-}15}$, were generally low. For these CDSs, even if numbers are statistically significant, biological consequences of such variations may be rather weak, if any (Tab. S2). Together, these observations indicated that the bulk gene reprogramming enabling the adaptation to σ^E induction occurred during the 10 first min, and a novel steady state was near to complete 20 min after σ^E induction.

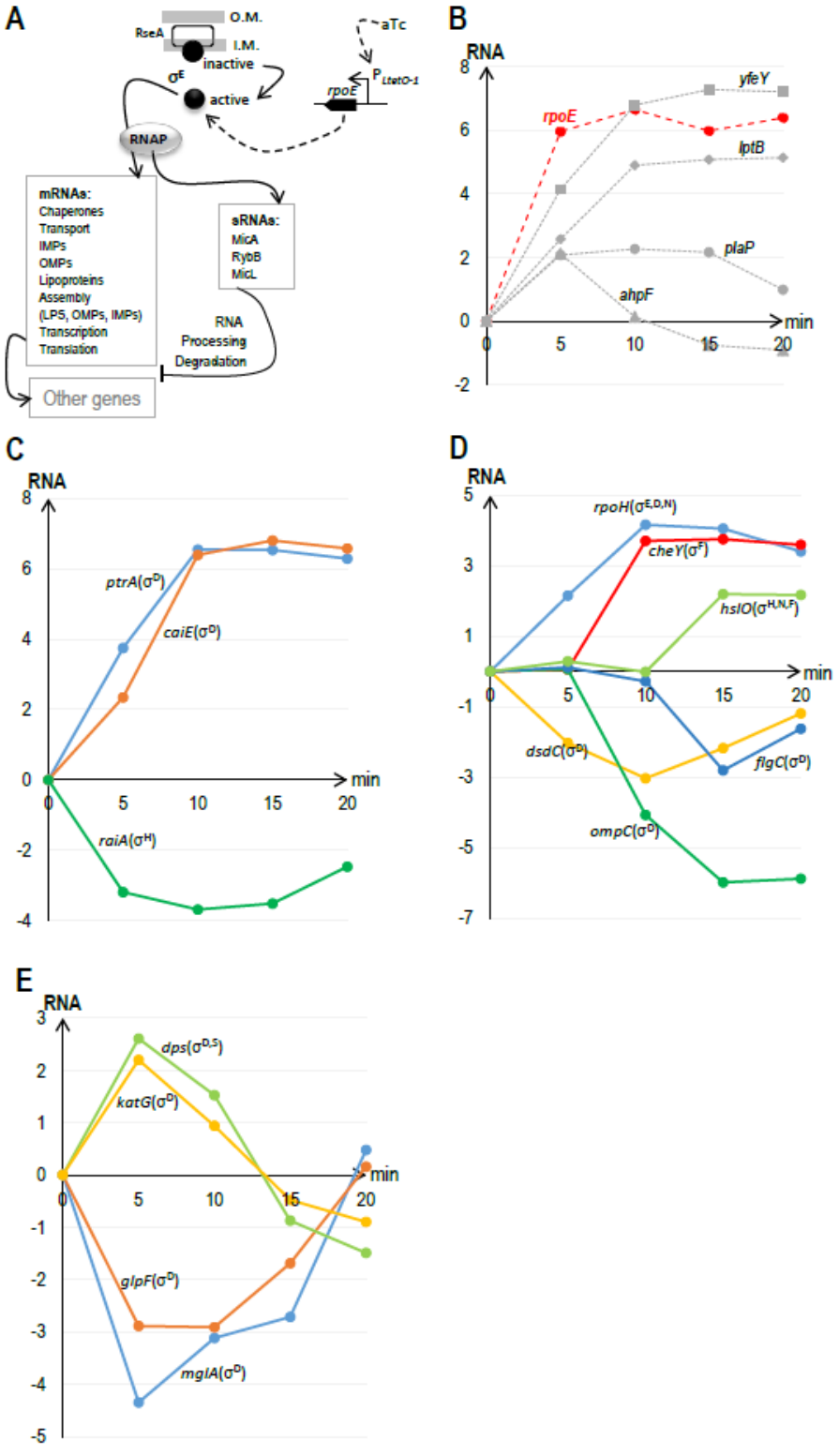

Figure S1. Experimental system used and examples of changes in RNA levels. A. Under non-stressful conditions, σ^E is inactive as it is sequestered by RseA at the inner membrane (I.M.). When the cell envelop homeostasis is disrupted, σ^E is released and binds to the RNAP that transcribes σ^E-dependent encoding sequences, including three sRNAs. In our experimental system, the σ^E encoding sequence, *rpoE*, is expressed from $P_{LtetO-1}$, induced by anhydrotetracycline (aTc). O.M.: Outer membrane. B. RNA levels of *rpoE* and others selected σ^E-dependent CDSs over the course of the experiment. C. Examples of early responding CDSs not transcribed by σ^E-RNAP. Sigma factors demonstrated or predicted to transcribe CDSs are indicated in parenthesis. D. Illustration of time-specific changes in RNA patterns. D. Examples of transient changes in RNA patterns. Y-axes (RNA): $\log_2$ of the ratio between RNA amounts at an experimental time point (t_i) and t_0. X-axes: Experimental time points (min). All numerical values are from Supplemental Tab. S2.

Genes transcribed by σ^E RNA polymerase

All CDSs demonstrated or predicted to be transcribed by σ^E-RNAP were retrieved within the kinetic interval t_{10-0} (Tab.S2) ((Rhodius et al. 2006; Mutalik et al. 2009; Keseler et al. 2017) and references therein). This proved that the induced *rpoE* mRNA encoded a functional σ^E. Among the 141 selected CDSs, 125 displayed increased levels at t_5 (87) or t_{10} (38) and mirrored the σ^E induction (Fig. 1B, Fig. S1B, Tab. S2). In contrast, the other 16 CDSs did not conform to the expected increased RNA pattern (Tab. S2). One of them, *ahpF*, selected at t_5, shows increased levels (~ 4-fold) and then fell at t_{15} and t_{20} to levels below the one measured at t_0. *ahpF* was demonstrated to be a σ^E-dependent transcripts (Rhodius et al. 2006), but its pattern suggested an increased RNA synthesis counter-balanced by an increased degradation (Fig. S1B). RNA levels for the other 15 CDSs displayed a pattern that disagree with a σ^E-dependent synthesis since their abundance decreased when the sigma factor was induced (Tab. S2). These CDSs have been predicted to be σ^E-dependent based on promoter predictions (Keseler et al. 2017), and it may that in our experimental conditions, their transcription was not controlled by σ^E-RNAP or that predictions were false. For instance, *mglC*, selected at t_5, showed a transient pattern (Tab. S2). Two σ^E-TSSs have been predicted for *mglC* within the upstream CDS *mglA*, in addition to the others upstream promoters σ^E-independent that drive the expression of *mglBAC* and *mglAC* operons (Keseler et al. 2017). CDSs *mglA* and *mglB* were also selected at t_5 and showed an expression that parallels the *mglC* pattern, favoring the speculation of an *mglAC* coexpression rather than a σ^E-dependent synthesis of *mglC*, independent of *mglAB* (Tab. S2).

Genes responding to σ^E induction but not transcribed by σ^E RNA polymerase

The expression of 560 additional CDSs, i.e. the majority of selected CDSs (~80 %), also displayed significant changes (Fig. 1B, Tab. S2). Their transcription is initiated by the RNAP associated with σ factors other than σ^E, i.e. σ^D, σ^H, σ^F, σ^N and σ^S (Keseler et al. 2017), and changes in RNA levels featured two distinct patterns.

a) The vast majority (500 CDs) increased or decreased their RNA levels relatively to t_0, and featured a novel steady state in less than 10 min. For instance, transcripts *caiE*, *csrD*, *ptrA*, *phoB* and *yabI* increased drastically within the first 5 min and their abundance reached a novel steady state by t_{10}. In an opposite manner, *malFG*, *napF*, *nupG* and *raiA* decreased sharply within the first 5 min (Fig. S1C, Tab. S2). The same pattern was also observed for RNAs whose levels changed after t_5 (Fig. S1D, Tab. S2). For instance, RNAs selected at t_{10}, *cheY*, *cbl*, *yfdQ* and *lpxM* showed drastic increased levels, and then, their abundances changed modestly by t_{15} and t_{20}. In the meantime, RNAs such as *flgC*, *gatBD*, *gnsA*, *gisB*, *msrC*, *proV* and *ymcE* displayed an opposite pattern. Although the bulk of reprogramming occurred during the first 10 min, these data illustrates the

temporal-specific expression of genes during the adaptation process induced by σ^E. Furthermore, since the transcription of these CDSs was not directly dependent on σ^E-RNAP, changes in RNA levels can be explained by: i) the competition between the increased amount of σ^E and other sigma factors for a limited amount of core-RNAP available, and ii) the expression of transcriptional and post-transcriptional regulators σ^E-dependent, including three sigma factors (σ^D, σ^N and σ^H) and sRNAs (Maeda et al. 2000; Dartigalongue et al. 2001; Rezuchova et al. 2003; Kabir et al. 2005; Rasmussen et al. 2005; Udekwu et al. 2005; Johansen et al. 2006; Rhodius et al. 2006; Udekwu and Wagner 2007; Bury-Mone et al. 2009; Rhodius and Mutalik 2010; De Vos et al. 2011; Gogol et al. 2011; Guo et al. 2014; Mauri and Klumpp 2014; Li et al. 2015).

b) The second group consisted of a minority of genes (60 out of 560) that showed transient changes in RNA levels, reminiscent of the *ahpF* pattern (Fig. S1B). We observed increased RNA levels followed by decreased amounts (e.g. *dps*, *grxA*, *katG*, *ndh*, *yhcN*), or the opposite (e.g. *dadAX*, *fxsA*, *glpABC*, *mglBA*, *sdhAB*). By t_{20}, these transcripts reached levels different or similar to those measured at t_0 (Fig. S1E, Tab. S2). Most likely, this group of transcripts illustrates antagonist controls involving RNA synthesis and RNA degradation where one effect tends to overcome the other (Esquerre et al. 2014).

sRNA-mediated controls depending on σ^E induction

σ^E-dependent sRNAs, MicA, RybB and MicL, base-pair mRNA targets and affect their degradation and/or their translation. 32 RNA targets have been predicted or demonstrated for MicA, RybB and MicL (Gogol et al. 2011; Guo et al. 2014). Drastic increased levels of these sRNAs were observed at t_5, and as a result, decreased levels for their cognate mRNAs were expected. Indeed, we observed decreased levels for 21 out of the 32 targets (Fig. S2, Tab. S3) (Gogol et al. 2011; Guo et al. 2014). RNA patterns indicated selectivity in the action of sRNAs and/or differential sensitivity of RNA targets. Among these 21 RNAs, 8 targets of MicA and/or RybB, behaved as expected: A decreased abundance was observed at t_5 and mirrored the increasing levels of sRNAs (*fimB*, *fumC*, *lamb*, *nmpC*, *ompF*, *ompW*, *rbsK* and *tsx*). Levels for the other 13 targets showed a significant decrease once MicA and RybB have reached more than 30- and 16-fold their original levels after t_5, respectively (i.e. *fimA*, *lpxT*, *fadL*, *gloA*, *ldtC*, *ompA*, *ompC*, *ompX*, *phoP*, *rbsB*, *rluD*, *rraB* and *ycfL*). In this group, a significant decreased for *rraB* was measured only after t_{10}. The differential effect of MicA and RybB on their cognate mRNAs suggests one group of targets sensitive to mild increases of sRNAs, and another that shows 'visible' degradation only when sufficient amounts of sRNAs are present in the cell (Fig. S2, Tab. S3). This observation illustrates the threshold effects mediated by sRNAs, i.e. the sRNA acts on its target once it reaches a sufficient amount (Levine et al. 2007). As consequence, within MicA- and RybB-regulons, the discrimination between targets suggests that in conditions imposing mild stresses and weak MicA and RybB variation levels, only a few mRNA targets would be controlled and the others would be unaffected.

Furthermore, 4 RNA targets of MicA, RybB and MicL were not significantly affected by σ^E induction, *asr*, *ecnB*, *lpp* and *ydeN* (Fig. S2, Tab. S3). The absence of sRNA effects may be due to differences in experimental systems used by others, no effect of sRNAs on the stability of mRNA targets or false predictions (Gogol et al. 2011; Guo et al. 2014). For instance, MicL displayed ~8- to 10-fold increased levels from t_5 onward, but *lpp*, the sole target demonstrated for MicL, did not show significant variations (Tab. S3), as reported by others

(Guisbert et al. 2007; Gogol et al. 2011).

In sharp contrast, 6 RNAs showed an increased level, a pattern incompatible with RNA-mediated degradation sRNA-dependent, *flu*, *yfeK*, *ygiM*, *yhjJ*, *pal* and *ybgF* (the two later CDSs are embedded in the same operon) (Fig. S2, Tab. S3). σ^E-dependent promoters have been predicted or mapped upstream *yfeK*, *ygiM* and *yhjJ* CDSs, and CHIP-seq experiments have shown the binding of σ^E-RNAP to *ygiM* and *yhjJ* promoter regions (Rhodius et al. 2006; Li et al. 2015; Keseler et al. 2017). These observations suggested that the increased *yfeK*, *ygiM* and *yhjJ* RNA levels resulted primarily from transcription, and the degradation effects mediated by MicA and RybB were minor, if any. Remarkably, it has been demonstrated that *yfeK*, *ygiM* and *yhjJ* RNA levels decreased when MicA and RybB were overexpressed ectopically (Gogol et al. 2011). Therefore, it may that additional mechanisms controlling the action of MicA and RybB on these targets occur when σ^E is induced; mechanisms otherwise absent when sRNAs are overexpressed in a σ^E-independent manner.

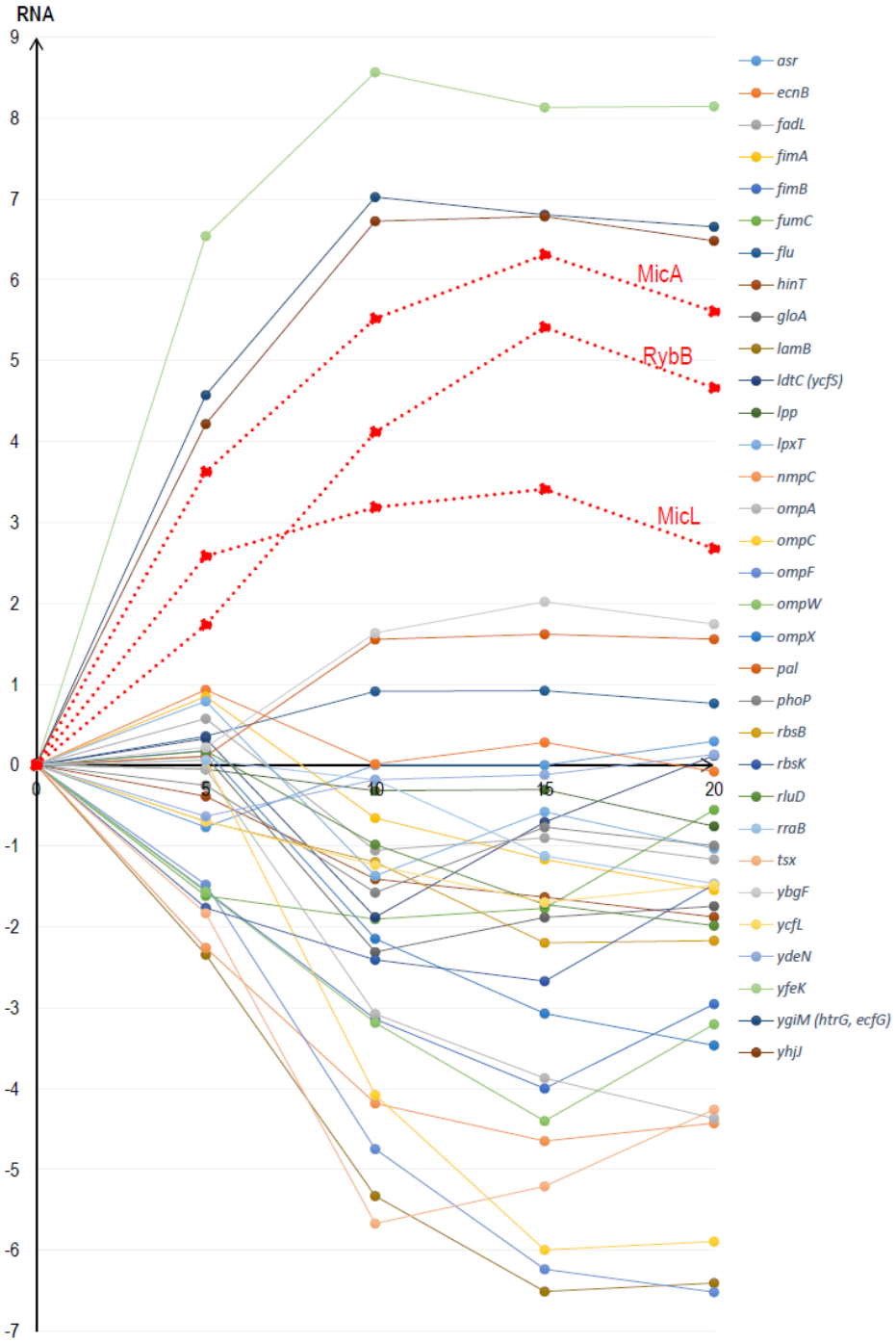

Figure S2. Patterns of sRNAs σ^E-dependent and their mRNA targets. Numerical values are from Tab. S3. Legends are otherwise identical to Fig. S2.

Section S2:

Assignment of 5’ RNA ends

For each transcriptome and each experimental time point, 5’ RNA ends were analyzed as previously defined (Innocenti et al. 2015). Briefly, a 5’ RNA end was considered mapped when at least 42 tags total were found in the 18 transcriptomes. As both TSS- and PSS-tags can ligate to the same RNA end, the ratio of tag-counts enables to define the value of an angle α, such as $\alpha = \arctan(n_{PSS}/n_{TSS})$, with n_{PSS} and n_{TSS} being PSS- and TSS-tag-counts, respectively (Tab. S4). According to the value of α, labels of 5’ RNA ends were defined: If $\alpha \leq 30°$, the 5’ RNA end was assigned as ‘TSS’; if $\alpha \geq 60°$, the 5’ RNA end was assigned as ‘PSS’; if $30° < \alpha < 60°$, the 5’ RNA end was undetermined (‘UND’).

Each 5’ RNA end has been mapped in three independent transcriptomes and in identical physiological states, resulting in three angles at each time point of the kinetics. When all three angles were in the same interval (i.e. $\leq 30°$, $\geq 60°$, or $30° < \alpha < 60°$), we kept the corresponding assignment. When angles were in different intervals, we assigned ‘UND’ to the 5’ end. By doing so, the labeling of a given 5’ RNA end can vary throughout the five experimental time points of the kinetics (TSS, PSS or UND). To sort out the definitive nature of each 5’ end, we applied two consecutive steps:

1) We assigned as TSS, 5’ ends displaying over the course of the experiment: 5 ‘TSSs’, 4 ‘TSSs’ + 1 ‘UND’, and 3 ‘TSSs’ + 2 ‘UND’. PSS RNA ends were assigned for situations: 5 ‘PSSs’, 4 ‘PSSs’ + 1 ‘UND’ and 3 ‘PSSs’ + 2 ‘UND’. Any other situation was assigned as ‘UND’.

2) For all ‘UND’ RNA ends, we analyzed the differential tagging between transcriptomes observed at t_0: The tobacco alkaline phosphatase (TAP) acts specifically on 5’-triphosphate RNA ends, therefore an increase of TSS-tag counts in TAP treated samples compared to TAP untreated samples strongly suggests the presence of a true TSS (Fig. 1A). Conversely, since PSSs are 5’-mono-phosphate termini and thus insensitive to the phosphatase, the TSS-tag count from a true PSS is expected to remain unchanged, regardless of the TAP treatment. Empirically, by estimating TSS-tag counts at each 5’ RNA end at t_0 from TAP-treated and untreated transcriptomes, we defined that a TAP treatment accompanied by at least 3-fold increase of TSS-tag counts indicated a true TSS. Thus, sensitivity to TAP at t_0 enabled us not only to confirm most of the assignments of TSS ends by the angle argument, but also to retrieve TSSs from the non-assigned population of ‘UND’ RNA ends.

Section S3: Figure S3. Patterns of changes in TIF at σ^E-TSSs assigned as UNDs or PSSs in this study.

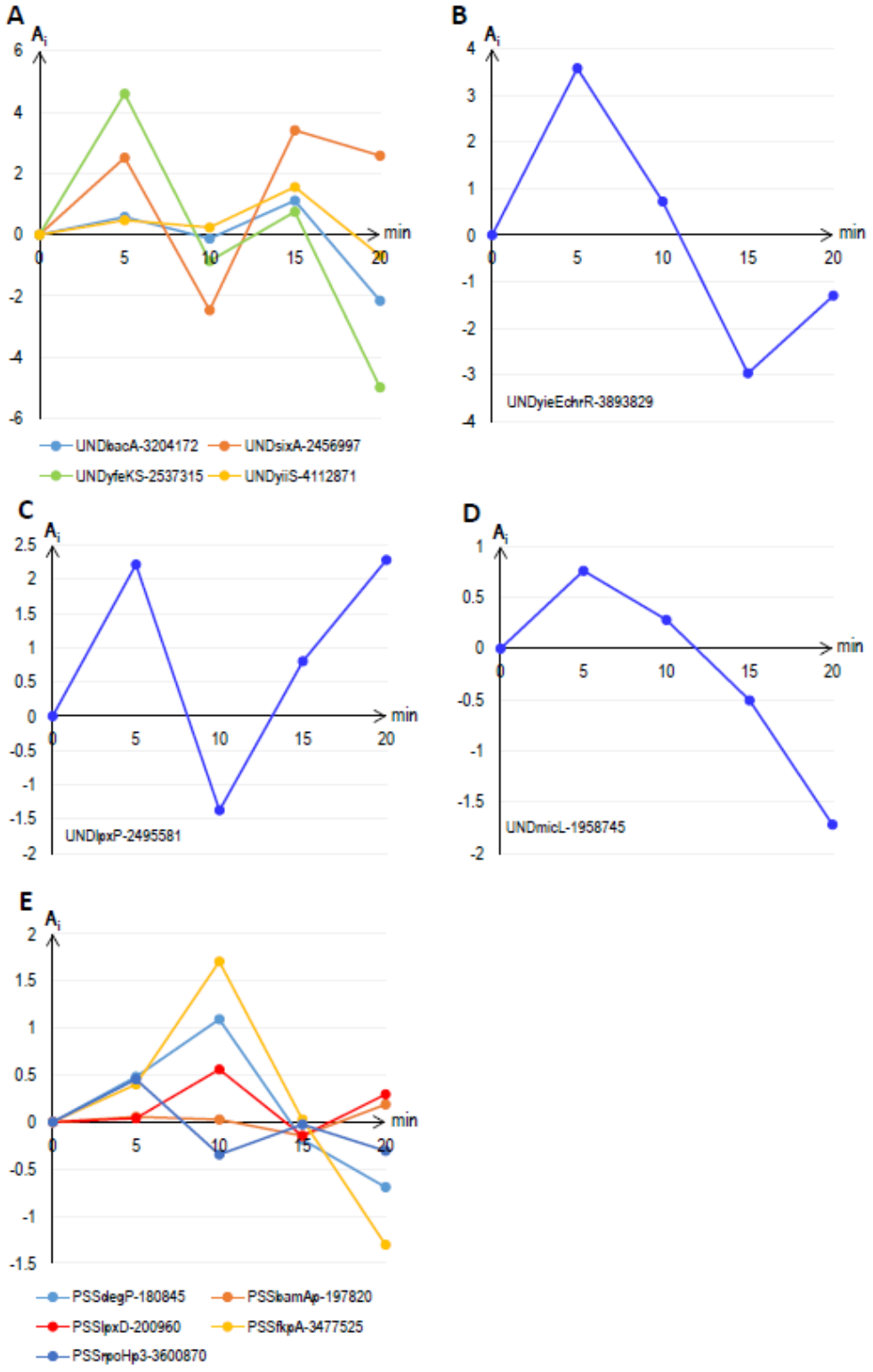

Figure S3. Patterns of changes in TIF at **σ**^{E}-TSSs assigned as UNDs (A, B, C, D) and PSSs (E) in this study. Legends are identical to Fig. 1.

Figure S4. Examples of changes in TIF at σ^E-independent TSSs

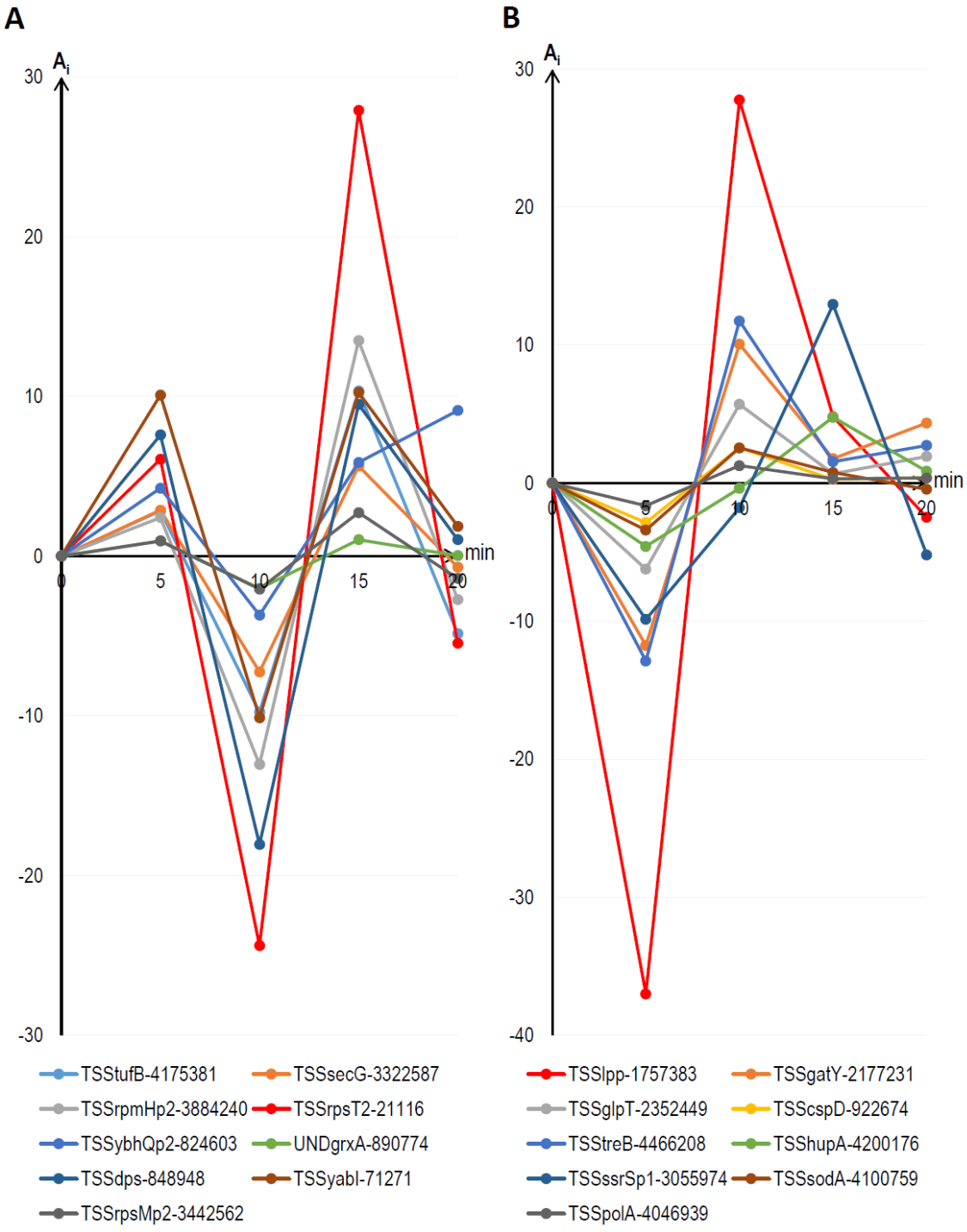

Figure S4. A. Transcription activation. B. Transcription repression. Heatmaps for selected examples are provided Fig. 2A and 2B. Legends are otherwise identical to Fig. 1.

Section S4: RNA dynamics at the *bepA-yfgD* operon

bepA encodes a chaperone/metalloprotease, and *yfgD*, a predicted oxireductase ((Keseler et al. 2017) and references on the website). We mapped the TSS of the operon at positions 2616066/69 (Fig. S5A), assigning the coordinate 2616068 as TSS, as previously reported (Rhodius et al. 2006). TSS-2616068 had a biphasic pattern that hallmarks transcription activation, an observation supported by the increased RNA levels measured under σ^E induction (Fig. 1C, 1F and Fig. S5B, S5C). Nine PSSs were assigned: Seven nested in *bepA* that are flanked by one in the 5'UTR (2616077) and another within the *yfgD* CDS (2617598) (Fig. S5A). Among those, only four PSSs in *bepA* showed significant changes in PFs. PSSs at coordinates 2617534 and 2617544 displayed modest and late PF variations in the interval $t_{20\text{-}15}$, possibly responding to RNA accumulation (Fig. S5B and S5D). In sharp contrast, PSSs at positions 2617541/2 showed earlier and more pronounced changes. However, these two PSSs featured distinct patterns, similarly to PSSs-312852/3 for *dnaG* (Fig. 3D). PSS-2617541 peaked at t_{10} and PSS-2617542 peaked at t_{15} (Fig. S5D), which suggests a different processing activity at these sites separated by 1 nt. PSS-2617541 displayed a progressive increased PF from t_0 that parallels the increased RNA pattern during the 10 first minutes, indicating an activity that responds to RNA synthesis and somehow to transcription activation. In contrast, for PSS-2617542, the onset of changes in PF occurred between t_5 and t_{10}, when *bepA-yfgD* RNA is reaching maximal amounts, suggesting a response to RNA accumulation (Fig. S5B, S5D). Thus, data suggest that PSS-2617541 alters the integrity of *bepA* as the bicistronic RNA is synthesized by responding to σ^E induction and mediating a differential expression to proteins encoded by the operon. This hypothesis agrees with a recent genome wide study in *E. coli* where the half-life of *yfgD* was estimated ~3-fold higher than *bepA* in steady state growth conditions (Dar and Sorek 2018).

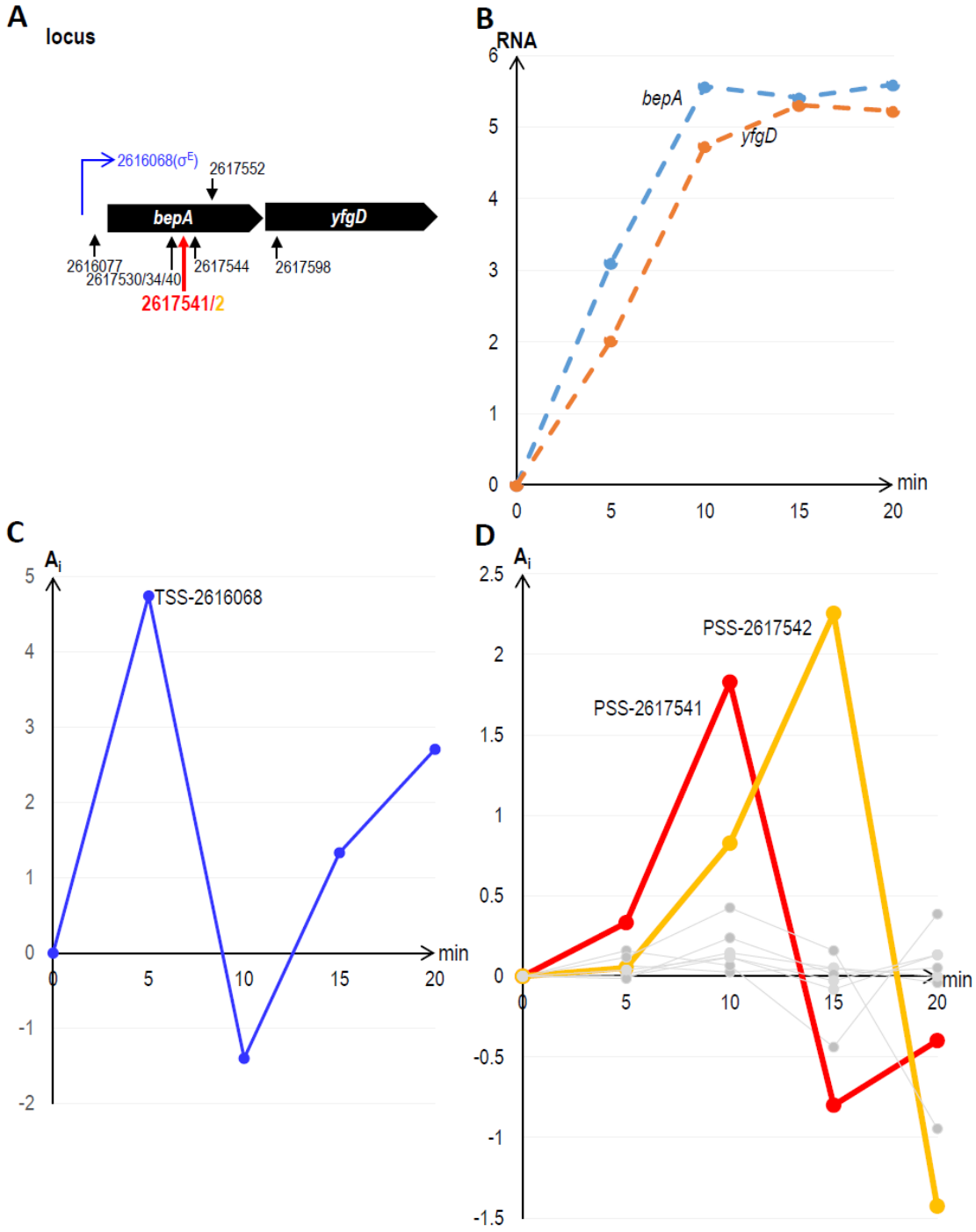

Figure S5. RNA dynamics at the *bepA-yfgD* locus. Legends are identical to Fig.3.

References

Bury-Mone S, Nomane Y, Reymond N, Barbet R, Jacquet E, Imbeaud S, Jacq A, Bouloc P. 2009. Global analysis of extracytoplasmic stress signaling in *Escherichia coli*. *PLoS Genet* **5**: e1000651.

Dar D, Sorek R. 2018. Extensive reshaping of bacterial operons by programmed mRNA decay. *PLoS Genet* **14**: e1007354.

Dartigalongue C, Missiakas D, Raina S. 2001. Characterization of the *Escherichia coli* sigma E regulon. *J Biol Chem* **276**: 20866-20875.

De Vos D, Bruggeman FJ, Westerhoff HV, Bakker BM. 2011. How molecular competition influences fluxes in gene expression networks. *PLoS One* **6**: e28494.

Esquerre T, Laguerre S, Furlan C, Carpousis AJ, Girbal L, Cocaign-Bousquet M. 2014. Dual role of transcription and transcript stability in the regulation of gene expression in *Escherichia coli* cells cultured on glucose at different growth rates. *Nucleic Acids Res* **42**: 2460-2472.

Gogol EB, Rhodius VA, Papenfort K, Vogel J, Gross CA. 2011. Small RNAs endow a transcriptional activator with essential repressor functions for single-tier control of a global stress regulon. *Proc Natl Acad Sci U S A* **108**: 12875-12880.

Guisbert E, Rhodius VA, Ahuja N, Witkin E, Gross CA. 2007. Hfq modulates the sigmaE-mediated envelope stress response and the sigma32-mediated cytoplasmic stress response in *Escherichia coli*. *J Bacteriol* **189**: 1963-1973.

Guo MS, Updegrove TB, Gogol EB, Shabalina SA, Gross CA, Storz G. 2014. MicL, a new sigmaE-dependent sRNA, combats envelope stress by repressing synthesis of Lpp, the major outer membrane lipoprotein. *Genes Dev* **28**: 1620-1634.

Innocenti N, Golumbeanu M, Fouquier d'Herouel A, Lacoux C, Bonnin RA, Kennedy SP, Wessner F, Serror P, Bouloc P, Repoila F et al. 2015. Whole-genome mapping of 5' RNA ends in bacteria by tagged sequencing: a comprehensive view in *Enterococcus faecalis*. *Rna* **21**: 1018-1030.

Johansen J, Rasmussen AA, Overgaard M, Valentin-Hansen P. 2006. Conserved small non-coding RNAs that belong to the sigmaE regulon: role in down-regulation of outer membrane proteins. *J Mol Biol* **364**: 1-8.

Kabir MS, Yamashita D, Koyama S, Oshima T, Kurokawa K, Maeda M, Tsunedomi R, Murata M, Wada C, Mori H et al. 2005. Cell lysis directed by sigmaE in early stationary phase and effect of induction of the *rpoE* gene on global gene expression in *Escherichia coli*. *Microbiology* **151**: 2721-2735.

Keseler IM, Mackie A, Santos-Zavaleta A, Billington R, Bonavides-Martinez C, Caspi R, Fulcher C, Gama-Castro S, Kothari A, Krummenacker M et al. 2017. The EcoCyc database: reflecting new knowledge about *Escherichia coli* K-12. *Nucleic Acids Res* **45**: D543-D550.

Levine E, Zhang Z, Kuhlman T, Hwa T. 2007. Quantitative characteristics of gene regulation by small RNA. *PLoS Biol* **5**: e229.

Li J, Overall CC, Johnson RC, Jones MB, McDermott JE, Heffron F, Adkins JN, Cambronne ED. 2015. ChIP-Seq Analysis of the sigmaE Regulon of *Salmonella enterica* Serovar Typhimurium Reveals New Genes Implicated in Heat Shock and Oxidative Stress Response. *PLoS One* **10**: e0138466.

Maeda H, Fujita N, Ishihama A. 2000. Competition among seven *Escherichia coli* sigma subunits: relative binding affinities to the core RNA polymerase. *Nucleic Acids Res* **28**: 3497-3503.

Mauri M, Klumpp S. 2014. A model for sigma factor competition in bacterial cells. *PLoS Comput Biol* **10**: e1003845.

Mutalik VK, Nonaka G, Ades SE, Rhodius VA, Gross CA. 2009. Promoter strength properties of the complete sigma E regulon of *Escherichia coli* and *Salmonella enterica*. *J Bacteriol* **191**: 7279-7287.

Rasmussen AA, Eriksen M, Gilany K, Udesen C, Franch T, Petersen C, Valentin-Hansen P. 2005. Regulation of *ompA* mRNA stability: the role of a small regulatory RNA in growth phase-dependent control. *Mol Microbiol* **58**: 1421-1429.

Rezuchova B, Miticka H, Homerova D, Roberts M, Kormanec J. 2003. New members of the *Escherichia coli* sigmaE regulon identified by a two-plasmid system. *FEMS Microbiol Lett* **225**: 1-7.

Rhodius VA, Mutalik VK. 2010. Predicting strength and function for promoters of the *Escherichia coli* alternative sigma factor, sigmaE. *Proc Natl Acad Sci U S A* **107**: 2854-2859.

Rhodius VA, Suh WC, Nonaka G, West J, Gross CA. 2006. Conserved and variable functions of the sigmaE stress response in related genomes. *PLoS Biol* **4**: e2.

Udekwu KI, Darfeuille F, Vogel J, Reimegard J, Holmqvist E, Wagner EG. 2005. Hfq-dependent regulation of OmpA synthesis is mediated by an antisense RNA. *Genes Dev* **19**: 2355-2366.

Udekwu KI, Wagner EG. 2007. Sigma E controls biogenesis of the antisense RNA MicA. *Nucleic Acids Res* **35**: 1279-1288.